QIRT'2022
10.21611/qirt.2022.2010
16th Quantitative InfraRed Thermography Conference

Quantification of CO2 passive degassing at sulphur Banks from Kilauea Volcano using thermal Infrared Multispectral Imaging.

by S. Boubanga Tombet* and E. Guyot*

* Telops, avenue St.-Jean-Baptiste, Québec (Québec) Canada G2E 6J5, *stephane.boubanga@telops.com*

Abstract

From volcanic emissions gases carbon dioxide (CO2) is generally the most abundant with the lowest solubility among the volatile compounds of magmatic liquids and the less susceptible than most other magmatic substances. Thus, volcanic CO2 emission rates could play an important role for constraining the role of magma degassing in the biogeochemical cycle of carbon. However, measurements of CO2 emission rates from volcanoes remain challenging, mainly due to the difficulty of measuring volcanic CO2 against the high level of CO2 in the atmosphere. In this work infrared multispectral imaging was used to identify and quantify volcanic carbon dioxide.

1. Introduction

Generally, volcano emissions contain significant proportions of water vapor (H2O) and carbon dioxide (CO2), along with variable proportions of toxic/corrosive gases such as sulphur dioxide (SO2), hydrogen chloride (HCl), hydrogen fluoride (HF), and silicon tetrafluoride (SiF4) [1]. Among those volcanic gas species, carbon dioxide is the least soluble in basaltic liquids [2]. Additionally, while the emissions of certain volcanic gas species such as SO2 may be lost totally due to their interactions with groundwater (hydrolysis of SO2 to aqueous H2S and sulphate for instance), carbon dioxide is less susceptible to scrubbing by water [3]. The scrubbing and solubility properties of CO2 underlines the importance of volcanic CO2 emission rates in the biogeochemical cycle of carbon on planet Earth, as well as its importance in the evaluation of volcanic hazards [4,5]. Measurements and quantification of CO2 emission rates from volcanoes remain challenging, mainly due to the presence of high background CO2 in the atmosphere [6]. Additional challenges are related to the unpredictable behaviour of volcanos and the life-threatening situations they may create to human lives and scientific instruments. Therefore, remote sensing measurements techniques are highly desirable for the investigation of volcanic gas species emission rates, including CO2. Among remote sensing techniques, thermal infrared imaging spectroscopy is particularly well-suited for the characterisation of volcanic activity, since many volcanic gases including CO2 and sulphur dioxide (SO2) are infrared-active molecules. In order to acquire spectral information using thermal infrared cameras, the spectral response of the camera can be tuned using, for instance, an interferometer-based infrared spectrometer (Telops Hyperspectral cameras) or spectral filters (Telops Multispectral camera). In the latter case, band-pass (BP), long-pass (LP) and high-pass (HP) spectral filters can readily be added to the camera optical path. Filter wheel systems allow for the storage of a selection of spectral filters readily available for acquisition. Multiple images of the same scene can thus be acquired using different spectral filters, representing a capability set that falls between high-speed broadband imaging and high-spectral resolution hyperspectral imaging. Spectral information is obtained from the response of individual spectral filters, ratios, subtractions and/or combinations of multiple filters. In general, a greater number of spectral bands provide more flexibility for challenging measurement situations.

When investigating volcanic gas emissions, high speed data acquisition ensures a high temporal resolution for the measurement. For this reason, the Telops MS-IR systems are equipped with a fast-rotating motorized filter wheel synchronized with image acquisition. Sequences are calibrated using in-band photon radiance (IBR) format, frame by frame, according to their respective spectral filter dataset. This allows the user to automatically collect frames on each spectral channel without having to handle and/or select filters manually. The Telops MS-, 5 LQIUDUHG FDPHUD¶V ILC allows storage of up to eight (8) different filters, providing enhanced flexibility over most filter wheel systems on the market. Due to its time-resolved capabilities and its spectral information, the MS system from Telops has proven to be particularly appropriate for gas cloud imaging [7].

In this work, gas detection and quantification measurements were conducted at the Sulphur Banks from Kilauea Volcano using a Telops MS-IR MW camera. All data was collected in in-band radiance format. A physical radiative transfer model was established to describe the contributions from all sources to the observed sensor signal. This radiative transfer model can be solved to obtain gas temperature and concentration at the individual pixel level.

Sulphur Banks is well known for continuous low-level emissions of volcanic gases along with groundwater steam. These gases are rich in carbon dioxide, sulphur dioxide and hydrogen sulphide. Measurements were carried out at a relatively high spatial resolution with bandpass spectral filters leading to successfully identification and quantification of carbon dioxide (CO2) from its distinct spectral features.

2. Experimental Information.

2.1. The multispectral camera

The camera used in this study (Figure 1) is a cooled high performance multispectral infrared (MS-IR) cameras available in different models covering the complete midwave and longwave infrared spectral ranges. The MS-IR MW (3 – 5 µm) and MS-IR VLW (7.7 – 11.8 µm) use indium antimonide (InSb), mercury-cadmium-telluride (MCT) or Strained Layer Superlattice (SLS) focal plane array (FPA) detectors with 320×256 or 640×512 pixels. The MS-IR HD is a MWIR camera which uses a high-definition 1280×1024 pixels FPA detector. The MS-IR infrared cameras allow the scene radiance to be split into eight (8) different spectral bands rather than only one broadband image, thereby providing spectral information about the investigated targets. The filter wheel is a fast-rotating mechanism designed to maximize the camera's frame rate and can be used either in fixed or rotating mode. The filter wheel is capable of reaching up to 6000 rpm, leading to a maximum effective frame rate of 800 Hz, i.e., up to 100 Hz per channel.

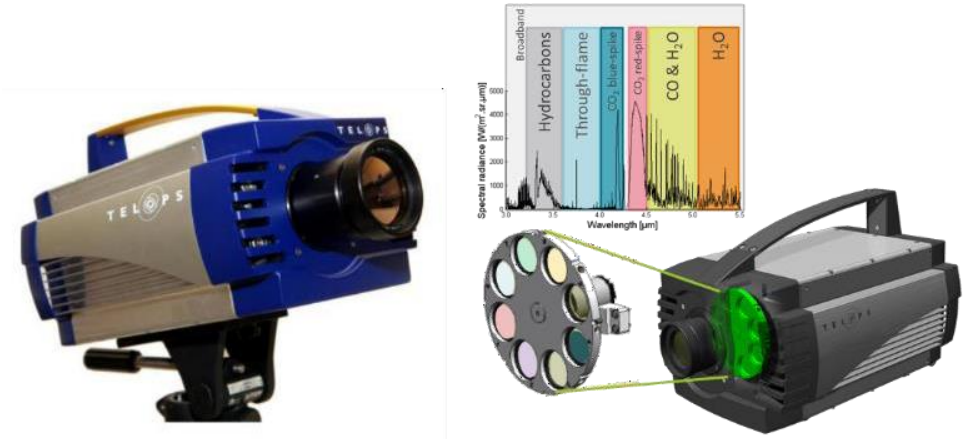

Fig. 1. *The Telops MS-IR camera (left) and the filter wheel system (right).*

2.2. Measurement configuration

The camera used for this measurement campaign is the MS-IR MW with spectral range covering between 3 to 4.9 µm. The filter configuration (Figure 2) consists of one sapphire window (filter #1) and one neutral density filter OD1 (filter #2) representative of the broadband channels and six spectral filters: BP 4665 nm, BW 240 nm (filter #3), BBP 4358-4534 nm (filter #4), BBP 3725-4245 nm (filter #5), BBP 3575-4125 nm (filter #6), BBP 3440-4075 nm (filter #7) and BBP 2900-3500 nm (filter #8). Acquisitions were carried out at full FPA frame (640×512 pixels) and the integration times were set between 300 and 6300 µs depending on the acquisition channel. Total acquisition frame rate was set to 80 Hz, which gives an effective frame rate of 10 Hz per channel. A MW optical lens of 50 mm was used and the distance between the camera and the target 2 m leading to a spatial resolution of 4 mm^2/pixel.

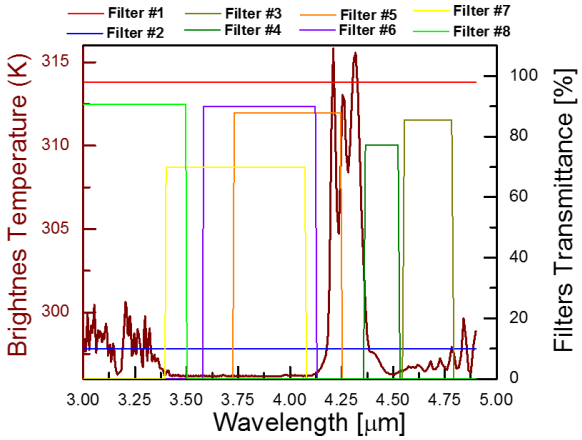

Fig. 2. MWIR spectrum of gas mixture shown in brightness temperature overlaid on the transmittance of the 8 spectral filters.

Figure 3 depicts the location of a borehole drilled in 1922 for underground heat measurements at Sulphur Banks. The Telops camera measuring volcanic gas exhausting form the borehole is also shown as well as a typical broadband IR image with the gas plume.

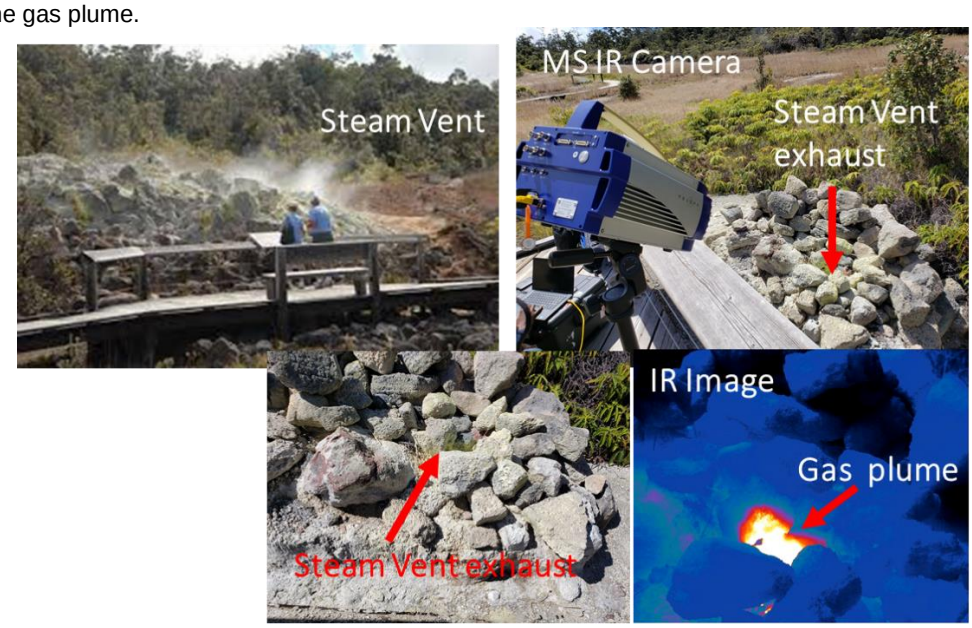

Fig. 3. Photographs of the experiment site, gas exhaust hole where measurements were conducted and a typical Broadband IR image of the gas plume.

2.3. Data Processing

A radiative transfer model was established to describe the phenomenology associated with the gas plume detection experiment using Equation 1:

$$L_{tot} = [L_{bkg}\tau_{gas} + L_{gas}(1-\tau_{gas})]\tau_{gas} + L_{atm}(1-\tau_{atm}) \quad (1)$$

where L corresponds to the radiance and τ corresponds to the transmittance. The background (bkg), the atmosphere (atm), and the gas from the plume (gas) are the main contributors to the total radiance ($Ltot$) measured at sensor level (see Figure 4). For the gas plume, only carbon dioxide was considered in this work due to the configuration of spectral filters available during measurements. We analysed data in terms of In-band radiance (IBR) which is determined by integrating the measured radiance over a defined spectral range (spectral filters). By combining the information from all spectral channels, IBR profiles are obtained for each pixel. Optimization of the equation above was carried out on the IBR profile of each pixel in order to estimate the gas plume temperature and its column density. The simulated IBR profiles were carried out using the HITRAN spectroscopic database.

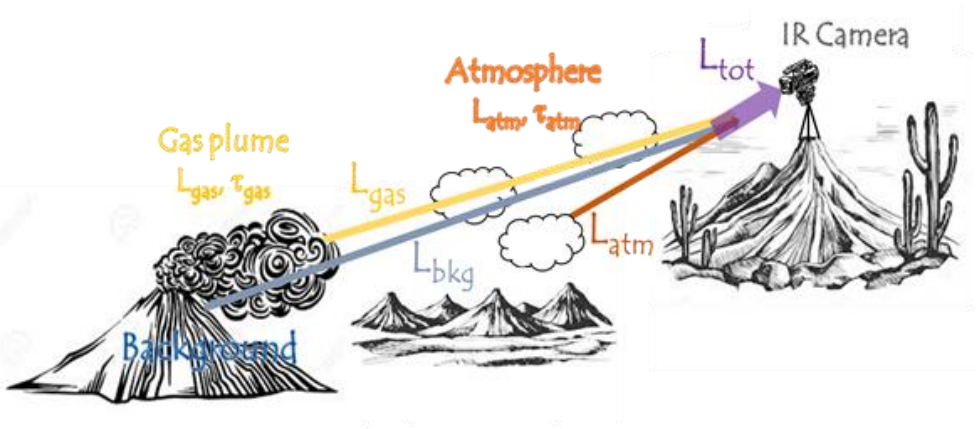

Fig. 3. Simplified radiative transfer model.

3. Results

At Sulphur Banks, volcanic water vapor seeps out of the ground mixed with volcanic gases mainly composed of carbon dioxide, sulphur dioxide and hydrogen sulphide. A representative MWIR brightness temperature spectrum of a representative gas mixture is depicted in Figure 2. The different spectral filters used during the measurement campaign are also shown for illustration purposes. The strong spectral features of CO2, seen between 4.15 and 4.5 µm, are associated with the C=O asymmetric stretch vibration. Some weak spectral features associated with water vapor can also be seen around 3.25 and 4.8 µm. Figure 5 shows selected acquisitions of the gas vent recorded through relevant spectral channels. Data from each frame was normalized using the IBR of a blackbody source at 20 °C. The most pronounced thermal contrasts for CO2 are obtained through filters #4 and #5 since the CO2 contribution to the signal observed through these filters is relatively high. The thermal contrast observed in the broadband channel (filter #1) is reduced compared to filters #4 and #5 because the relative contribution to the total signal due to CO2 emission is reduced. The thermal contrast observed in filters #3 and #8 are attributed to water vapor. Very small contrasts associated gases exhaust can be seen through the other filters (see filters #7) which can be useful for obtaining information about the background radiance. Such information is necessary for accurate estimation of the gas temperature and concentration using the radiative transfer model discussed above.

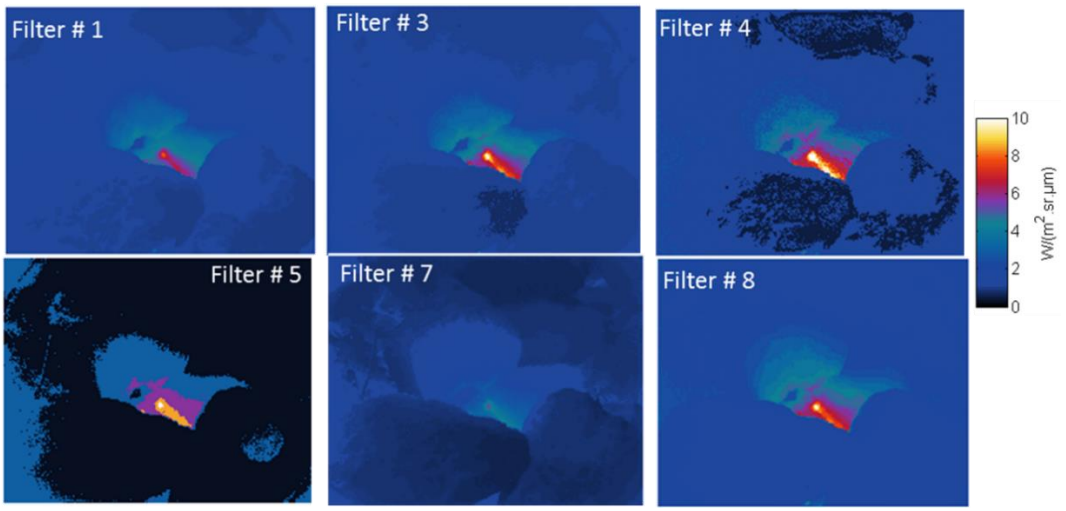

Fig. 5. *Normalized responses (blackbody at 20 °C) of selected relevant acquisition channel for multispectral imaging experiment on volcanic gas vent.*

3.1. IBR-profile optimization

A typical IBR profile associated with the volcanic gas emission is shown in Figure 6. Broadband imagery does not allow the user to resolve the chemical nature of targets in the investigated scene due to the lack of spectral information. Comparing the signal obtained in different channels (Fig. 5) with the MS camera in terms of thermal contrast already gives an additional level of information about the chemical nature of the gases seeping out of the borehole. However, thermal contrast would only allow qualitative spectral analysis since the detector response in a single channel is function of many parameters and subject to interfering agents. In order to unambiguously identify and quantify the gases emanating from the borehole, Equation 1 was used to fit the measurement data (See Fig. 6). The IBR profile is computed by integrating the Planck curve equation over the spectral range of each filter. The IBR of a selected target can be estimated for each filter according to its spectral emissivity/transmittance for defined gas concentration and thermal contrast conditions. Selected gas concentration can then be estimated by correlating the estimated IBR profile with measured IBR profiles of individual pixels in a scene. The gas thermodynamic temperature and transmittance are therefore retrieved allowing estimation of gas concentration.

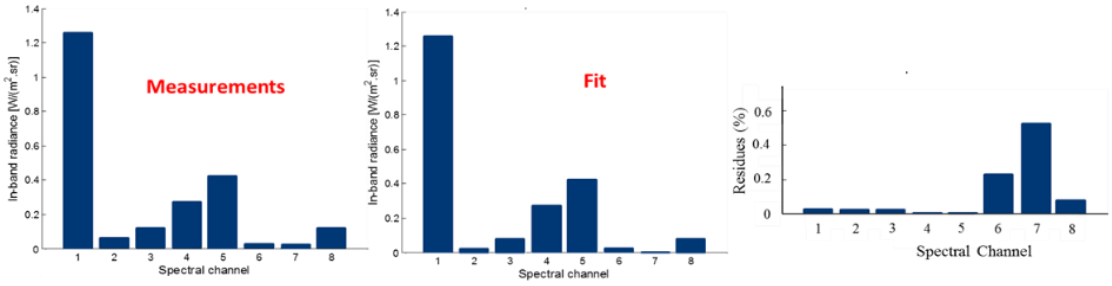

Fig. 6. *Typical measured and Fit In-band radiance (IBR) profiles.*

3.2. Gas Quantification

3.2.1. Gas concentration

The column density of CO2 maps of four different acquisitions are shown on Fig. 7. Quantification was performed by fitting the radiative transfer model (Equation 1) with a non-linear optimization routine in order to estimate the relative contribution of each parameter of the equation to the total measured radiance signal. The gas transmittance τ_{gas} = exp(-$\Sigma\kappa l\rho$) in Eq.1 is function of gas concentration ρ (expressed in ppm), path length l (expressed in meters) and the gas molar absorptivity κ. CO2 gas column density values of up to 35 ppm.m were obtained around the investigated exhaust hole. When the dimensions of the plume are known, the column density path length dependence can be factorized in order to retrieve the gas concentration ρ in ppm. Figure 8 depicts the maximum local CO2 concentration versus acquisition time at two different locations near the vent hole. The red and blue line on the top left panel of Fig.7 show the locations where the local concentrations were estimated.

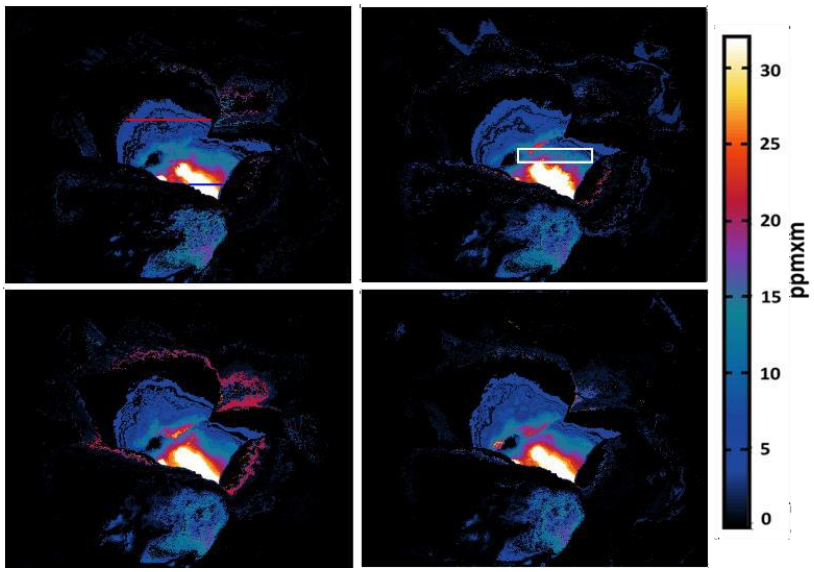

Fig. 7. *CO2 Column density extracted for measurements using Eq.1*

The contribution of background CO2 in the atmosphere was taken into account in τatmalong with the other atmospheric gas species such as N2O and water vapor. Concentrations of several hundreds of ppm were observed in the vicinity of the exhaust hole, dropping down to a few tens of ppm approximately 10 cm away, most likely due to the wind spreading and diluting the gas into the atmosphere.

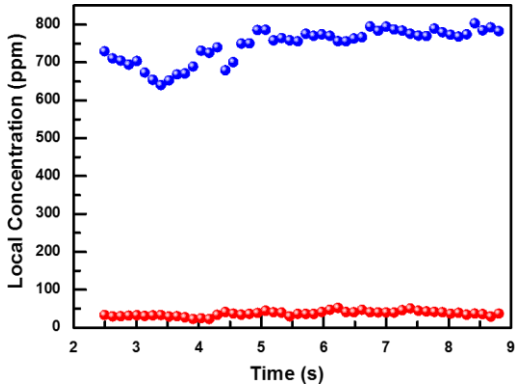

Fig. 8. *CO2 Local concentration in vicinity of the exhaust hole (bleu dotes) and 10 cm away (red dotes).*

3.2.2. Velocity Estimation using Optical Flow

A dynamic flow analysis based on a pixel per pixel temporal radiance variation technique was carried out to estimate the gas cloud velocity [8]. The mean velocity maps obtained for selected acquisitions are shown in Figure 9. The red arrows correspond to local velocity vectors of different orientations and magnitudes. Gas cloud velocities of several m/s were obtained. Wind speed velocity can also be obtained from local meteorological data.

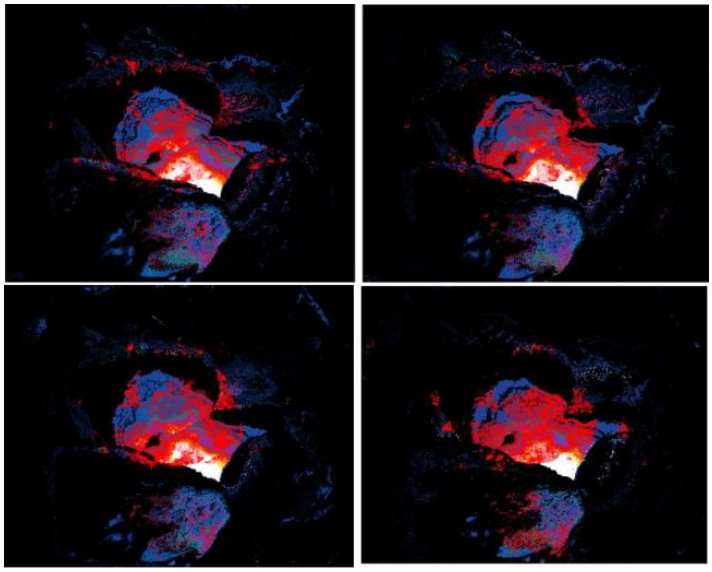

Fig. 9. *Local velocity map obtained after optical flow analysis displayed over the infrared image for clarity purposes.*

3.2.3. Mass density

From the path length concentration results (Fig.7), we calculate the CO2 mass density within a specified area of the image using Equation 2.

$$m = \sum c \times d \times \sigma_{gas} \qquad (2)$$

where c is the gas path length concentration (ppm.m), d is the pixel size (m), σgas is the gas density (g/m3). Total CO2 mass of 87 mg was obtained within the area of interest shown in white on the top right panel of Fig.7.

3.2.4. Mass Flow Rates

The mass flow rate (flux) in g/s is calculated using the average mass density in a selected area and the mean gas velocity as shown in Equation 3.

$$F = m \times v \qquad (3)$$

where m is the mass density, and $\boldsymbol{v}$ is the mean gas velocity or wind speed. Figure 10 shows the estimated CO2 mass flow rate obtained for different acquisitions. The estimated values fluctuate significantly from acquisition to acquisition most likely due to changing wind conditions. Good knowledge of wind parameters is essential to improve the precision of the quantification results. Variability and uncertainties on the flow rate estimation may come from the concentration map and linear mass density estimation depending on the precision of the fit of data with Eq.1. Uncertainties may also originate from the gas cloud velocity estimation.

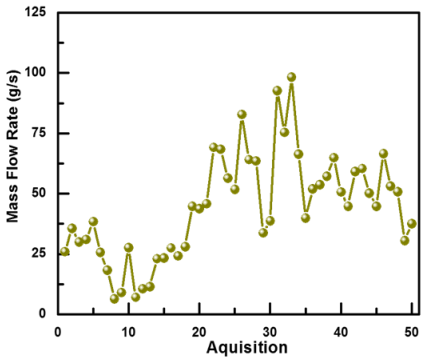

Fig. 10. *CO2 mass flow rate estimates as a function of time.*

4. Conclusion

Time-resolved multispectral imaging allows efficient investigation of passive or active volcanic degassing. The Telops multispectral imaging system provides spectral information without sacrificing the imaging frame rate required in such situations. IBR profiles drawn from 8 acquisition channels provide good spectral selectivity. The additional information brought by dynamic multispectral imaging over conventional thermal cameras brings new possibilities for infrared signature measurements. Our methodology produces CO2 column density measurements within the volcano's plume which are used to estimate CO2 concentration. Quantitative chemical maps with local CO2 concentrations of hundreds of ppm were derived and corresponding mass flow rates of tens g/s were also estimated. The results show that thermal infrared multispectral imaging can provide unique insights for volcanology studies.

REFERENCES

[1] Symonds, R. B., W. I. Rose, G. J. S. Bluth, and T. M. Gerlach, Volcanic gas studies: Methods, results, and applications, in Volatiles in Magma, Reviews in Mineralogy, vol. 30, edited by M. R. Carroll and J. R. Holloway, 1-66, Mineralogical Society of America, Washington, D.C., (1994).

[2] Holloway, J. R., and J. G. Blank, Application of experimental results to C-O-H species in natural melts, in Volatiles in Magma, Reviews in Mineralogy, vol. 30, edited by M. R. Carroll and J. R. Holloway, 187-230, Mineralogical Society of America, Washington, D.C., (1994).

[3] Doukas M. P., and T. M. Gerlach, Sulfur dioxide scrubbing during the 1992 eruptions of Crater Peak, Mount Spurr volcano, Alaska, in U.S. Geol. Surv. Bull., 2139, 47-57, (1995).

[4] Berner, R . A., Global CO2 degassing and the carbon cycle: Comment on "Cretaceous ocean crust at DSDP sites 417 and 418: Carbon uptake from weathering vs. loss by magmatic outgassing," Geochim. Cosmochim. Acta, 54, 2889-2890, (1990).

[5] Gerlach, T. M., H. Delgado, K. A. McGee, M.P. Doukas, J. J. Venegas, and L. Cardenas, Application of the LI-COR CO2 analyzer to volcanic plumes: A case study, volcan Popocatepetl, Mexico, June7 and 10, 1995, J. Geophys Res.,102, 8,005-8,019, (1997).

[6] Andres, R. J., and W. I. Rose, Remote sensing spectroscopy of volcanic plumes and clouds, in Monitoring Active Volcanoes, edited by McGuire, B., C. Kilburn, and J. Murray, pp. 301-314, UCL Press Ltd., London, (1995).

[7] Marc-André Gagnon, Karl-Alexandre Jahjah, Frédéric Marcotte, Pierre Tremblay, Vincent Farley and Martin Chamberland. "Time-resolved thermal infrared multispectral imaging of gases and minerals," Proc. of SPIE 9249, (2010)

[8] Horn, B.K.P., Schunck, B.G., Determining Optical Flow, 17, 185-203 (1981).